Theor Chem Account (2008) 120:199–213
DOI 10.1007/s00214-007-0322-6

REGULAR ARTICLE

Spectral-product methods for electronic structure calculations

P. W. Langhoff · R. J. Hinde · J. D. Mills · J. A. Boatz

Received: 5 December 2006 / Accepted: 9 April 2007 / Published online: 12 June 2007

Abstract Progress is reported in development, implementation, and application of a spectral method for ab initio studies of the electronic structure of matter. In this approach, antisymmetry restrictions are enforced subsequent to construction of the many-electron Hamiltonian matrix in a complete orthonormal spectral-product basis. Transformation to a permutation-symmetry representation obtained from the eigenstates of the aggregate electron antisymmetrizer is seen to enforce the requirements of the Pauli principle ex post facto, and to eliminate the unphysical (non-Pauli) states spanned by the product representation. Results identical with conventional use of prior antisymmetrization of configurational state functions are obtained in applications to many-electron atoms. The development provides certain advantages over conventional methods for polyatomic molecules, and, in particular, facilitates incorporation of fragment information in the form of Hermitian matrix representatives of atomic and diatomic operators which include the non-local effects of overall electron antisymmetry. An exact atomic-pair expression is obtained in this way for polyatomic Hamiltonian matrices which avoids the ambiguities of previously described semi-empirical fragment-based methods for electronic structure calculations. Illustrative applications to the well-known low-lying doublet states of the H_3 molecule in a minimal-basis-set demonstrate that the eigensurfaces of the antisymmetrizer can anticipate the structures of the more familiar energy surfaces, including the seams of intersection common in high-symmetry molecular geometries. The calculated H_3 energy surfaces are found to be in good agreement with corresponding valence-bond results which include all three-center terms, and are in general accord with accurate values obtained employing conventional high-level computational-chemistry procedures. By avoiding the repeated evaluations of the many-centered one- and two-electron integrals required in construction of polyatomic Hamiltonian matrices in the antisymmetric basis states commonly employed in conventional calculations, and by performing the required atomic and atomic-pair calculations once and for all, the spectral-product approach may provide an alternative potentially efficient ab initio formalism suitable for computational studies of adiabatic potential energy surfaces more generally.

Keywords Potential energy surfaces · Ab initio calculations · Electronic states · Spectral methods · Antisymmetry constraints

Contribution to the Mark S. Gordon 65th Birthday Festschrift Issue.

P. W. Langhoff (✉)
San Diego Supercomputer Center,
University of California San Diego, 9500 Gilman Drive,
MS 0505, La Jolla, CA 92093-0505, USA
e-mail: langhoff@drifter.sdsc.edu

R. J. Hinde
Department of Chemistry, University of Tennessee,
Knoxville, TN 37996-1600, USA

J. D. Mills · J. A. Boatz
Air Force Research Laboratory, 10 East Saturn Blvd.,
Edwards AFB, CA 93524-7680, USA

1 Introduction

Considerable progress has been reported over the past four decades in ab initio studies of the complex (Born–Oppenheimer) potential energy surfaces which describe the ground and low-lying excited electronic states of molecules [1]. The contributions of Professor Mark S. Gordon to this enterprise have been remarkably comprehensive, as typified by his central role in the development, wide-spread

distribution, and continuing collaborative refinement of the well-known GAMESS suite of computer codes [2]. Accurate ab initio methods provided in this and other computational resources for potential energy surfaces commonly entail repeated calculations of large numbers of one- and two-electron multicentered integrals over explicitly antisymmetrized basis states in construction of a many-electron Hamiltonian matrix for a range of atomic spatial arrangements, followed by determinations of the energies and associated eigenfunctions of selected electronic states at each atomic arrangement, and construction of the expectation values corresponding to physical properties of interest. New methods for these purposes devised in a spirit of continuing collaborative improvements would clearly be welcome, particularly if they could avoid repeated calculations of the individual electronic integrals and related quantities generally required in the construction of potential energy surfaces, or possibly circumvent entirely the determinations of total molecular energies (and their associated differencing problems) in favor of calculations of atomic and interaction energies, while still proving applicable to both ground and electronically excited states on a common basis.

In a contribution to the systematic improvement of standard quantum-chemical methods, an alternative perspective is provided in the present report on enforcement of the antisymmetry requirement on proper atomic and molecular wave functions [3–11], which requirement is commonly satisfied by the aforementioned prior constraint on the representational basis states employed in variational calculations [1, 2]. In the present approach, rather, Pauli's exclusion principle is ignored at the outset, and antisymmetry is enforced subsequent to construction of the Hamiltonian matrix in a spectral-product representational basis familiar from the theory of long-range interactions [12]. When applied to the electronic structures of atoms as an introductory pedagogical example, the development is seen to be equivalent to the familiar Slater approach adopting prior antisymmetry of many-electron configurational states functions [13], providing some degree of confidence in the alternative method more generally. In applications to polyatomic molecules, the approach provides a number of advantages over conventional methods, and, in particular, accommodates the incorporation of ab initio atomic and diatomic information in polyatomic Hamiltonian matrices in a rigorous manner which avoids certain difficulties encountered in previously described semi-empirical fragment-based approaches [14,15].

The present method is ultimately based on conventional variational calculations in L^2 representations of many-electron states, guaranteeing its convergence when closure is achieved, in which limit distinctions between use of simple-product and explicitly antisymmetrized aggregate basis states are known to become formally inconsequential. As presented here, the theory is applicable to polyatomic molecules which dissociate into neutral species on their lowest lying potential energy surfaces, but which can otherwise involve arbitrary admixtures of covalent, ionic, van der Waals, and metallic interatomic interactions. Applications of the approach to ionic systems, or to neutral systems which can give rise to ion-pair states in asymptotic separation limits, require only minor, largely self-evident, modifications of the present description.

The atomic spectral-product basis employed in the development is known to span the totally antisymmetric irreducible representation of the aggregate electron symmetric group once and only once, making it suitable for analytical and computational studies of the electronic structures of many-electron systems [16–20]. A matrix representative of the antisymmetrizer constructed in the spectral-product basis is employed in separating the totally antisymmetric and non-totally-antisymmetric (non-Pauli) states spanned by the basis, and in correspondingly isolating the physically significant block of the Hamiltonian matrix by unitary transformation. Hermitian matrix representations of atomic and atomic-pair operators are devised in this way for polyatomic molecules which individually have well-defined asymptotic separation limits, and which need be constructed only once for multiple applications. These attributes of the approach facilitate development of an ab initio unitary transformation formalism which provides the aforementioned exact atomic-pair representation of polyatomic Hamiltonian matrices, including particularly the important modifications of the bare atomic-pair interactions due to the aggregate electron antisymmetry required upon incorporation into the polyatomic system.

The general theory is presented in Sect. 2, where the spectral-product representation of electrons is defined and the unitary transformation formalism for isolating the physical portion of the Hamiltonian is described for both atoms and molecules. Strategies for computational implementation of the method are addressed in Sect. 3, including in particular description of the atomic-pair implementation and illustrative calculations of the low-lying doublet electronic states of the H_3 molecule. Concluding remarks summarizing the salient features of the approach are given in Sect. 4.

2 Theory

The spectral-product approach to the electronic structures of atoms is described in Sect. 2.1 as a pedagogical introduction to the formalism, whereas its application to polyatomic molecules is presented in Sect. 2.2.

2.1 Spectral-product formalism for atomic structure

Solutions of the Schrödinger equation [21]

$$\hat{H}(\boldsymbol{r})\boldsymbol{\Psi}(\boldsymbol{r}) = \boldsymbol{\Psi}(\boldsymbol{r}) \cdot \mathbf{E} \tag{1}$$

for an n-electron atom with Hamiltonian operator [22]

$$\hat{H}(\boldsymbol{r}) = \sum_{i=1}^{n} \Big\{ -\frac{\hbar^2}{2m}\nabla_i^2 - \frac{Ze^2}{r_i} + \sum_{j=i+1}^{n} \frac{e^2}{r_{ij}} \Big\} \tag{2}$$

can be constructed employing a formally complete square-integrable (L^2) representation in the outer-product form [16]

$$\boldsymbol{\Phi}(\boldsymbol{r}) = \{\boldsymbol{\phi}(\mathbf{1}) \otimes \boldsymbol{\phi}(\mathbf{2}) \otimes \cdots \boldsymbol{\phi}(\boldsymbol{n})\}_O \,. \tag{3}$$

The row vector $\boldsymbol{\phi}(\boldsymbol{i})$ employed in Eq. (3) comprises a denumerable finite or infinite basis set of orthonormal one-electron spin-orbitals specified by the usual quantum numbers (n, l, m_l, s, m_s) [22], where $\boldsymbol{i}$ refers to the spin and space coordinates of the ith electron and $\boldsymbol{r} \equiv (\mathbf{1}, \mathbf{2}, \ldots, \boldsymbol{n})$ represents collectively the coordinates of all n atomic electrons. The particular choice of spin-orbitals is irrelvant for the present development, so long as the outer-product ($\otimes$) Hilbert space of Eq. (3) can include a suitable closure in the limit of a complete spectral basis [23]. The subscript "O" in Eq. (3) indicates the adoption of a particular ordering convention for the sequence of product functions in the row vector $\boldsymbol{\Phi}(\boldsymbol{r})$, the consequences of which convention are indicated when appropriate in the sequel.

The Hamiltonian matrix representative of the operator of Eq. (2) in the basis of Eq. (3),

$$\begin{aligned}\mathbf{H} &\equiv \langle \boldsymbol{\Phi}(\boldsymbol{r}) | \hat{H}(\boldsymbol{r}) | \boldsymbol{\Phi}(\boldsymbol{r}) \rangle \\ &= \sum_{i=1}^{n} \Big\{ \mathbf{T}^{(i)} + \mathbf{V}^{(i)} + \sum_{j=i+1}^{n} \mathbf{V}^{(i,j)} \Big\},\end{aligned} \tag{4}$$

includes kinetic $\mathbf{T}^{(i)} \equiv \langle \boldsymbol{\Phi}(\boldsymbol{r}) | -(\hbar^2/2m)\nabla_i^2 | \boldsymbol{\Phi}(\boldsymbol{r}) \rangle$, potential $\mathbf{V}^{(i)} \equiv \langle \boldsymbol{\Phi}(\boldsymbol{r}) | Ze^2/r_i | \boldsymbol{\Phi}(\boldsymbol{r}) \rangle$, and electron-interaction $\mathbf{V}^{(i,j)} \equiv \langle \boldsymbol{\Phi}(\boldsymbol{r}) | e^2/r_{ij} | \boldsymbol{\Phi}(\boldsymbol{r}) \rangle$ Hermitian matrix representatives of the corresponding operators. The dimensions of these matrices are determined by that of the many-electron basis of Eq. (3), although only standard one and two-electron integrals, and their products with the unit matrices expressing the orthonormality of the remaining $n-1$ and $n-2$ orbitals, respectively, are required in evaluations of the Hamiltonian matrix of Eq. (4). The specific forms of these matrices are determined by the particular ordering convention adopted in Eq. (3) [16].

The matrix Schrödinger equation [21]

$$\mathbf{H} \cdot \mathbf{U_H} = \mathbf{U_H} \cdot \mathbf{E} \tag{5}$$

provides approximate or exact representations of the row vector of eigenfunctions of Eq. (1) in the form $\boldsymbol{\Psi}(\boldsymbol{r}) = \boldsymbol{\Phi}(\boldsymbol{r}) \cdot \mathbf{U_H}$, as well as the diagonal matrix of associated eigenvalues $\mathbf{E}$. The energy eigenspectrum so obtained includes both physically significant (totally antisymmetric) and unphysical (non-totally antisymmetric or non-Pauli) solutions, all of which are spanned by the representation of Eq. (3) [17]. Accordingly, this particular representation, and the corresponding Hamiltonian matrix and Schrödinger equation of Eqs. (4) and (5), can encompass descriptions of the electrons as either Bose–Einstein, Fermi–Dirac, or possibly other forms of identical particles, necessitating some means of distinguishing among these possibilities [24].

The physical and non-Pauli eigenstates obtained from Eqs. (1)–(5) can be separated by constructing a transformed Hamiltonian matrix which has a physical block, a non-Pauli block, and vanishing off-diagonal blocks. This separation is accomplished by constructing the eigenstates of the n-electron antisymmetrizer in the representation of Eq. (3) and transforming the Hamiltonian matrix of Eq. (4) to this new representation. The required representation matrix is

$$\mathbf{P_A} \equiv \langle \boldsymbol{\Phi}(\boldsymbol{r}) | \hat{P}_A(n) | \boldsymbol{\Phi}(\boldsymbol{r}) \rangle, \tag{6}$$

where the n-electron Hermitian antisymmetrizer employed [24],

$$\hat{P}_A(n) \equiv \sum_{p=1}^{n!} (-1)^{\delta_p} \hat{P}_p, \tag{7}$$

is left unnormalized. Alternatively, adoption of wavefunction or idempotent normalization in Eq. (7), which conventions require the familiar prefactors $(1/n!)^{1/2}$ and $(1/n!)$, respectively, does not materially affect the ensuing development, except for multiplicative changes of the spectral interval in which the eigenvalues of the antisymmetrizer are placed.

The matrix of Eq. (6) is found to comprise a series of individual non-zero $n!$-by-$n!$ blocks on the diagonal, the elements of which are all either $+1$ or -1, and a remaining set of vanishing blocks. The dimensions, numbers, and natures of the non-zero blocks of the $\mathbf{P_A}$ matrix are deteremined by the number of distinct spin-orbital products employed in the representation of Eq. (3), and by the presence of all $(n!)$ permutations of electrons among these products. This structure ensures that any finite atomic representation in the form of Eq. (3) provides an invariant subspace such that the operation of the antisymmetrizer is closed in this subspace

$$\hat{P}_A(n) \boldsymbol{\Phi}(\boldsymbol{r}) = \boldsymbol{\Phi}(\boldsymbol{r}) \cdot \mathbf{P_A}. \tag{8}$$

As a consequence, the eigenfunctions of the matrix representative of the antisymmetrizer in any such finite space will transform correctly as either totally antisymmetric or non-totally antisymmetric basis states under all electron permutations [24].

The eigenvalues and eigenfunctions of the antisymmetrizer are obtained in the usual way from the unitary transformation matrix $\mathbf{U_P}$ that diagonalizes the matrix of Eq. (6),

$$\mathbf{U_P^\dagger} \cdot \mathbf{P_A} \cdot \mathbf{U_P} = \begin{pmatrix} n!\,\mathbf{I}_{pp} & \mathbf{0}_{pu} \\ \mathbf{0}_{up} & \mathbf{0}_{uu} \end{pmatrix}, \tag{9}$$

where the physical block $n!\,\mathbf{I}_{pp}$ contains the non-zero eigenvalues and the unphysical $\mathbf{0}_{uu}$ and off-diagonal blocks vanish identically. The individual non-zero $n!$-by-$n!$ blocks of $\mathbf{P_A}$ indicated above are each diagonalized separately and contribute a single non-vanishing eigenvalue ($n!$) each to the physical block of Eq. (9). All other eigenvalues of $\mathbf{P_A}$ are identically zero, and correspond to the non-totally-antisymmetric states spanned by the product representation of Eq. (3).

The eigenfunctions of the antisymmetrizer take the correspondingly blocked form

$$\mathbf{\Phi_P}(\boldsymbol{r}) \equiv \mathbf{\Phi}(\boldsymbol{r}) \cdot \mathbf{U_P} = \left\{ \{\mathbf{\Phi_P}(\boldsymbol{r})\}_p, \{\mathbf{\Phi_P}(\boldsymbol{r})\}_u \right\}, \tag{10}$$

consequent of the ordering of the columns of the $\mathbf{U_P}$ matrix implied by Eq. (9), where the physical states satisfy

$$\hat{P}_A(n)\{\mathbf{\Phi_P}(\boldsymbol{r})\}_p = n!\,\{\mathbf{\Phi_P}(\boldsymbol{r})\}_p \tag{11}$$

and the non-Pauli states provide the null results $\hat{P}_A(n)\{\mathbf{\Phi_P}(\boldsymbol{r})\}_p = \mathbf{0}$. It is found by construction that the physical eigenstates of Eqs. (10) and (11) are linearly independent Slater determinants made up of the products of spin-orbitals of Eq. (3) which can provide totally antisymmetric states, whereas the non-Pauli eigenstates are totally symmetric, or are linear combinations of other (degenerate) representations of the nth-degree symmetric group [24]. The number of such spin-orbital products leading to non-vanishing Slater determinants times $n!$ gives the dimension of the physical block $\mathbf{I}_{pp}$ appearing in Eq. (9).

Equations (6)–(11) indicate that the spectrum of $\hat{P}_A(n)$ acting in the domain of the spectral-product basis of Eq. (3) is that of a compact operator [25], the value zero providing a lower limiting point of accumulation of the spectrum of eigenvalues, with $\{\mathbf{\Phi_P}(\boldsymbol{r} : \boldsymbol{R})\}_u$ the associated eigenstates. The totally antisymmetric states $\{\mathbf{\Phi_P}(\boldsymbol{r} : \boldsymbol{R})\}_p$ and associated eigenvalues $n!$ correspond to the upper limiting point of the allowable spectral interval $(0, n!)$.

The unitary matrix of Eq. (9) provides a transformed Hamiltonian matrix in the form

$$\mathbf{H_P} \equiv \mathbf{U_P^\dagger} \cdot \mathbf{H} \cdot \mathbf{U_P} = \begin{pmatrix} \{\mathbf{H_P}\}_{pp} & \mathbf{0}_{pu} \\ \mathbf{0}_{up} & \{\mathbf{H_P}\}_{uu} \end{pmatrix}, \tag{12}$$

where $\{\mathbf{H_P}\}_{pp}$ and $\{\mathbf{H_P}\}_{uu}$ are the physical (pp) and unphysical (uu) blocks which provide the totally antisymmetric and the non-Pauli solutions, respectively, and the off-diagonal blocks vanish identically in accordance with Eqs. (8) and (10). The physical Hamiltonian matrix of Eq. (12) is identical with that obtained from the linearly independent Slater determinants constructed by selecting only ordered spin-orbital configurations from the basis of all such products of Eq. (3). Accordingly, the transformation matrix $\mathbf{U_P}$ of Eq. (9) obtained from the matrix representative of the antisymmetrizer of Eq. (6) incorporates the effects of electron permutation symmetry, in the absence of prior basis-set antisymmetry in Eq. (3), in the Hamiltonian matrix of Eq. (4) through the transformation of Eq. (12).

2.2 Spectral-product formalism for polyatomic molecules

The foregoing spectral-product formalism for many-electron atoms also applies with some important differences and modifications to the adiabatic (Born–Oppenheimer) electronic structures of polyatomic molecules. Specifically, in the molecular case all quantities given in Sect. 2.1 depend explicitly upon the spatial arrangement of atoms in the molecule, specified by the vector $\boldsymbol{R} \equiv (\boldsymbol{R}_1, \boldsymbol{R}_2, \ldots, \boldsymbol{R}_n)$, where $\boldsymbol{R}_\alpha$ gives the position of the atom α. In order to follow closely the atomic development of Sect. 2.1, and to avoid unnecessary notational complexity, the molecular development is presented here for a collection of n one-electron (hydrogen) atoms [17], with generalization to many-electron atoms requiring only minor additional elaboration [20].

The spectral-product representation of Eq. (3) for polyatomic H_n molecules becomes

$$\mathbf{\Phi}(\boldsymbol{r} : \boldsymbol{R}) = \left\{ \boldsymbol{\phi}^{(1)}(\boldsymbol{1}) \otimes \boldsymbol{\phi}^{(2)}(\boldsymbol{2}) \otimes \cdots \boldsymbol{\phi}^{(n)}(\boldsymbol{n}) \right\}_O, \tag{13}$$

where the indvidual spectral states $\boldsymbol{\phi}^{(\alpha)}(\boldsymbol{i})$ are the one-electron spin-orbital row vectors of Eq. (3), with the electron coordinates $\boldsymbol{i}$ now measured relative to the different atomic origins $\boldsymbol{R}_\alpha$. As in the case of Eq. (3), the basis of Eq. (13) spans the totally antisymmetric representation of the aggregate n-electron permutation group once and only once, as well as all other (non-Pauli) representations of the nth-degree symmetric group, in the limit of closure [17].

The molecular Hamiltonian operator for a collection of n interacting hydrogen atoms can be written in the form [cf., Eq. (2)]

$$\begin{aligned} \hat{H}(\boldsymbol{r} : \boldsymbol{R}) &\equiv \sum_{\alpha=1}^{n} \left\{ \hat{H}^{(\alpha)}(\boldsymbol{i}) + \sum_{\beta=\alpha+1}^{n} \hat{V}^{(\alpha,\beta)}(\boldsymbol{i}, \boldsymbol{j} : \boldsymbol{R}_{\alpha\beta}) \right\} \\ &= \sum_{\alpha=1}^{n} \left\{ \left\{ -\frac{\hbar^2}{2m} \nabla_{i\alpha}^2 - \frac{e^2}{r_{i\alpha}} \right\} \right. \\ &\quad \left. + \sum_{\beta=\alpha+1}^{n} \left\{ \frac{e^2}{R_{\alpha\beta}} - \frac{e^2}{r_{i\beta}} - \frac{e^2}{r_{j\alpha}} + \frac{e^2}{r_{ij}} \right\} \right\}, \end{aligned} \tag{14}$$

where electron $i\,(j)$ is arbitrarily assigned to the atomic center at $\boldsymbol{R}_\alpha$ ($\boldsymbol{R}_\beta$), employing common notational conventions [21]. A decomposition of the aggregate Hamiltonian operator similar to that of Eq. (14) is also possible for interacting many-electron atoms, although sums over the electrons i and j assigned to the atoms α and β are, of course, required in this case [16].

The matrix representative of the operator of Eq. (14) constructed in the basis of Eq. (13) [cf., Eq. (4)],

$$\mathbf{H}(\boldsymbol{R}) \equiv \langle \boldsymbol{\Phi}(\boldsymbol{r} : \boldsymbol{R}) | \hat{H}(\boldsymbol{r} : \boldsymbol{R}) | \boldsymbol{\Phi}(\boldsymbol{r} : \boldsymbol{R}) \rangle = \sum_{\alpha=1}^{n} \Big\{ \mathbf{H}^{(\alpha)} + \sum_{\beta=\alpha+1}^{n} \mathbf{V}^{(\alpha,\beta)}(\boldsymbol{R}_{\alpha\beta}) \Big\}, \tag{15}$$

is seen to include atomic terms $\mathbf{H}^{(\alpha)} \equiv \langle \boldsymbol{\Phi}(\boldsymbol{r} : \boldsymbol{R}) | \hat{H}^{(\alpha)}(\boldsymbol{i}) | \boldsymbol{\Phi}(\boldsymbol{r} : \boldsymbol{R}) \rangle$ and atomic-pair interaction terms $\mathbf{V}^{(\alpha,\beta)}(\boldsymbol{R}_{\alpha\beta}) \equiv \langle \boldsymbol{\Phi}(\boldsymbol{r} : \boldsymbol{R}) | \hat{V}^{(\alpha,\beta)}(\boldsymbol{i}; \boldsymbol{j} : \boldsymbol{R}_{\alpha\beta}) | \boldsymbol{\Phi}(\boldsymbol{r} : \boldsymbol{R}) \rangle$ which provide Hermitian matrix representatives of the corresponding atomic and interaction operators. The atomic energy matrix $\mathbf{H}^{(\alpha)}$ is independent of atomic position and includes only diagonal one-electron energies when the orthonormal atomic spin-orbitals $\boldsymbol{\phi}^{(\alpha)}(\boldsymbol{i})$ are chosen to be atomic pseudo-eigenstates, whereas the interaction matrix $\mathbf{V}^{(\alpha,\beta)}(\boldsymbol{R}_{\alpha\beta})$ is generally non-diagonal and depends explicitly upon the vector separation $\boldsymbol{R}_{\alpha\beta}$ of the two indicated atoms, but not upon the individual laboratory-frame positions of the two atoms, nor upon the position vectors of the other $(n-2)$ atoms in the molecule. Evaluation of the particularly simple Hamiltonian matrix of Eq. (15) evidently requires only one-center atomic and two-center Coulombic interaction terms, which can be determined once and for all and retained for repeated applications. These favorable circumstances are consequences of the orthonormality of the spectral-product basis employed in the absence of prior enforcement of overall electron antisymmetry, the adoption of atomic pseudo-states in the representation, and the atomic pairwise-additive nature of the interaction terms in the Hamiltonian operator of Eq. (14).

Following the development of Sect. 2.1, the Hermitian matrix representative of the antisymmetrizer $\hat{P}_A(n)$ of Eq. (7) constructed in the basis of Eq. (13),

$$\mathbf{P}_\mathbf{A}(\boldsymbol{R}) \equiv \langle \boldsymbol{\Phi}(\boldsymbol{r} : \boldsymbol{R}) | \hat{P}_A(n) | \boldsymbol{\Phi}(\boldsymbol{r} : \boldsymbol{R}) \rangle = (n!)^{-1} \langle \hat{P}_A(n) \boldsymbol{\Phi}(\boldsymbol{r} : \boldsymbol{R}) | \hat{P}_A(n) \boldsymbol{\Phi}(\boldsymbol{r} : \boldsymbol{R}) \rangle, \tag{16}$$

is seen to depend explictly on the atomic arrangement $\boldsymbol{R}$, and to be proportional to the so-called metric matrix of the explicitly antisymmetrized product basis [21]. In contrast to the atomic matrix of Eq. (6), the matrix of Eq. (16) is a potentially complicated function of $\boldsymbol{R}$, requiring detailed computational evaluation. Moreover, the operation of the antisymmetrizer is not closed in any finite representation of the form of Eq. (13), and requires a complete spectral representation to achive closure as a limiting process $\hat{P}_A(n)\boldsymbol{\Phi}(\boldsymbol{r} : \boldsymbol{R}) \rightarrow \boldsymbol{\Phi}(\boldsymbol{r} : \boldsymbol{R}) \cdot \mathbf{P}_\mathbf{A}(\boldsymbol{R})$ [cf., Eq. (8)]. This circumstance is a consequence of the fact that, in contrast to the situation in the atomic case of Eq. (3), the representation of Eq. (13) does not include explicitly all $n!$ permutations of electron assignments to the indicated spin-orbital product states. That is, in contrast to standard treatments [10,24], in which "symmetrical" or "democratic" representations of all electrons are employed, the representation of Eq. (13) employs different spin-orbital basis sets to describe the different electrons arbitrarily assigned to each atom, since these basis sets are centered at different atomic positions $\boldsymbol{R}_\alpha$. Accordingly, electron permutations are included in Eq. (13) only implictly in the limit of a complete spin-orbital representation.

The unitary transformation matrix $\mathbf{U}_\mathbf{P}(\boldsymbol{R})$ required to partition the Hamiltonian matrix of Eq. (15) into physical and non-Pauli blocks is obtained from the diagonalization [cf., Eq. (9)]

$$\mathbf{U}_\mathbf{P}(\boldsymbol{R})^\dagger \cdot \mathbf{P}_\mathbf{A}(\boldsymbol{R}) \cdot \mathbf{U}_\mathbf{P}(\boldsymbol{R}) = \begin{pmatrix} \{\mathbf{P}_\mathbf{d}(\boldsymbol{R})\}_{pp} & \mathbf{0}_{pu} \\ \mathbf{0}_{up} & \{\mathbf{P}_\mathbf{d}(\boldsymbol{R})\}_{uu} \end{pmatrix} \rightarrow \begin{pmatrix} n!\,\mathbf{I}_{pp} & \mathbf{0}_{pu} \\ \mathbf{0}_{up} & \mathbf{0}_{uu} \end{pmatrix}. \tag{17}$$

Here, the eigenvalues of the matrix $\mathbf{P}_\mathbf{A}(\boldsymbol{R})$ are partitioned into an upper diagonal block $\{\mathbf{P}_\mathbf{d}(\boldsymbol{R})\}_{pp}$ containing the largest eigenvalues which tend to the upper limiting point $n!$ of the spectrum in the closure limit, and a lower diagonal block $\{\mathbf{P}_\mathbf{d}(\boldsymbol{R})\}_{uu}$ of eigenvalues which tend to the point of accumulation at zero in this limit [17–20]. Similarly, the permutation-symmetry-adapted eigenstates of the antisymmetrizer are obtained in this case as a limit in the form [cf., Eq. (10)]

$$\boldsymbol{\Phi}_\mathbf{P}(\boldsymbol{r} : \boldsymbol{R}) \equiv \boldsymbol{\Phi}(\boldsymbol{r} : \boldsymbol{R}) \cdot \mathbf{U}_\mathbf{P}(\boldsymbol{R}) \rightarrow \big\{ \{\boldsymbol{\Phi}_\mathbf{P}(\boldsymbol{r} : \boldsymbol{R})\}_p, \{\boldsymbol{\Phi}_\mathbf{P}(\boldsymbol{r} : \boldsymbol{R})\}_u \big\}, \tag{18}$$

where $\{\boldsymbol{\Phi}_\mathbf{P}(\boldsymbol{r} : \boldsymbol{R})\}_p$ contains the totally antisymmetric states corresponding to the non-zero eigenvalues $[\{\mathbf{P}_\mathbf{d}(\boldsymbol{R})\}_{pp} \rightarrow n!\,\mathbf{I}_{pp}]$ of the antisymmetrizer, and $\{\boldsymbol{\Phi}_\mathbf{P}(\boldsymbol{r} : \boldsymbol{R})\}_u$ contains the non-Pauli states corresponding to the zero eigenvalues $[\{\mathbf{P}_\mathbf{d}(\boldsymbol{R})\}_{uu} \rightarrow \mathbf{0}_{uu}]$ of the antisymmetrizer, in accordance with Eq. (17). Of course, the partionings of Eqs. (17) and (18) can be somewhat subjective in any finite representation, in contrast to the situation in Eqs. (9)–(12), where invariant physical and non-Pauli subspaces are obtained even in finite atomic representations, consequent of Eq. (8).

Finally, the unitary matrix $\mathbf{U}_\mathbf{P}(\boldsymbol{R})$ of Eq. (17) is employed in constructing the transformed Hamiltonian matrix

$$\begin{aligned} \mathbf{H}_\mathbf{P}(\boldsymbol{R}) &\equiv \mathbf{U}_\mathbf{P}(\boldsymbol{R})^\dagger \cdot \mathbf{H}(\boldsymbol{R}) \cdot \mathbf{U}_\mathbf{P}(\boldsymbol{R}) \\ &= \sum_{\alpha=1}^{n} \Big\{ \mathbf{H}_\mathbf{P}^{(\alpha)}(\boldsymbol{R}) + \sum_{\beta=\alpha+1}^{n} \mathbf{V}_\mathbf{P}^{(\alpha,\beta)}(\boldsymbol{R}) \Big\} \\ &= \begin{pmatrix} \{\mathbf{H}_\mathbf{P}(\boldsymbol{R})\}_{pp} & \{\mathbf{H}_\mathbf{P}(\boldsymbol{R})\}_{pu} \\ \{\mathbf{H}_\mathbf{P}(\boldsymbol{R})\}_{up} & \{\mathbf{H}_\mathbf{P}(\boldsymbol{R})\}_{uu} \end{pmatrix} \\ &\rightarrow \begin{pmatrix} \{\mathbf{H}_\mathbf{P}(\boldsymbol{R})\}_{pp} & \mathbf{0}_{pu} \\ \mathbf{0}_{up} & \{\mathbf{H}_\mathbf{P}(\boldsymbol{R})\}_{uu} \end{pmatrix}, \end{aligned} \tag{19}$$

where $\mathbf{H}_\mathbf{P}^{(\alpha)}(\boldsymbol{R})$ and $\mathbf{V}_\mathbf{P}^{(\alpha,\beta)}(\boldsymbol{R})$ refer to transformations of the individual atomic and interaction matrices in Eq. (15), $\{\mathbf{H}_\mathbf{P}(\boldsymbol{R})\}_{pp}$ and $\{\mathbf{H}_\mathbf{P}(\boldsymbol{R})\}_{uu}$ are the physical (pp) and unphysical (uu) blocks of the transformed Hamiltonian

matrix which provide the antisymmetric and the non-Pauli solutions, respectively, and the off-diagonal blocks vanish in the limit ($\rightarrow$) of spectral closure [17–20]. The transformation of Eq. (19) is seen to incorporate the non-local effects of overall electron antisymmetry in the atomic $\mathbf{H}^{(\alpha)} \rightarrow \mathbf{H}_{\mathbf{P}}^{(\alpha)}(\boldsymbol{R})$ and interaction $\mathbf{V}^{(\alpha,\beta)}(\boldsymbol{R}_{\alpha\beta}) \rightarrow \mathbf{V}_{\mathbf{P}}^{(\alpha,\beta)}(\boldsymbol{R})$ matrices, which consequently now depend on the positions of all atoms in the molecule. The Hermitian atomic and pair-interaction matrices of Eq. (19) individually have appropriate dissociation limits, with the entire Hamiltonian matrix approaching the sum of the individual atomic terms of Eq. (15) in the complete dissociation limit $\boldsymbol{R} \rightarrow \infty$, consequent of the absence of electron exchange in this limit $[\mathbf{P}_{\mathbf{A}}(\boldsymbol{R} \rightarrow \infty) \rightarrow \mathbf{I}]$ in the denumerable L^2 representation of Eq. (13) [20].

3 Computational implementation and application

Aspects of computational implementation and numerical application of the spectral-product formalism made to date are summarized in Sect. 3.1. The atomic-pair-based variant of the approach is reported in Sect. 3.2, and illustrative numerical applications of the new method to the low-lying doublet states of the H_3 molecule are given in Sect. 3.3.

3.1 Implementation strategies

The Hamiltonian matrices of Eqs. (15) and (19) related by the unitary transformation matrix of Eq. (17) provide identical energy eigenvalues and eigenfunctions which converge to those of the operator of Eq. (14) in the limit of closure of the spectral-product representation of Eq. (13). A number of strategies devised for verifying the ideas and theorems on which the spectral-product development is based, and for determining the desired Hamiltonian eigenspectra, has been employed to date in selected cases [16–20]. Brief descriptions of progress made in these approaches aid in understanding the issues which must be overcome in devising a generally applicable computational implementation of the spectral-product formalism.

Although computations based directly on Eq. (15), which entail only evaluations of the indicated atomic and atomic-pair interaction terms, appear attractive, previously described technical complications associated with the presence of unphysical continua, spuriously degenerate solutions, and slow convergence in long-range separation limits mitigate against adopting such an approach in general [20]. In the special case of two-electron systems, however, the electron spin functions can be factored out, the remaining allowable spatial wave functions are either symmetric or antisymmetric under transposition of the electron coordinates, and unphysical (non-Pauli) or spuriously degenerate solutions are not present. Accordingly, computational studies of the H_2 molecule based on Eqs. (13)–(15) can be performed in appropriately chosen orbital-product basis sets, the results of which exhibit monotone convergence with basis set expansion to the well-known lowest lying singlet and triplet energies [18]. Examination of the electronic charge densities of these states clarifies the manner in which the spectral-product representation can describe the accumulation or depletion of negative charge between the atoms relative to the undisturbed atomic charge distributions, providing thereby chemical bonding or anti-bonding in the two states entirely in the absence of commonly employed classical chemical structures to describe the wave functions [18]. Additionally, the expectation values of the electron transposition operator $\hat{P}_{ij}$ employing the singlet and triplet spectral-product wave functions are seen to converge smoothly with basis set expansion to the appropriate values ($\pm$ 1) in each case [18]. These results provide confidence in the development of Eqs. (13)–(15) in applications to the prototypically important electron pair bond.

Evaluations of the $\mathbf{P}_{\mathbf{A}}(R)$ matrix of Eq. (16) for the H_2 molecule in appropriately chosen basis sets over the range $R \leq 10\, a_0$ of atomic separation verify the convergence of the eigenvalues of Eq. (17) to the upper ($n! \rightarrow 2$) and lower (0) end points of the allowed spectral interval in this case [19, 20]. Construction of the transformed Hamiltonian matrix of Eq. (19) verifies the blocking indicated there, corresponding to separation of the singlet and triplet states in the absence of unphysical representations in this two-electron case. Furthermore, the rate at which the off-diagonal blocks of the Hamiltonian matrix which potentially connect the two different spin symmetries become negligible with increasing basis is made quantitative in the calculations [19,20].

As an alternative to constructing the unitary transformation matrix of Eq. (17) and the Hamiltonian matrix of Eq. (19) for the H_2 molecule, the representation of Eq. (13) is augmented with explicitly antisymmetric Heitler-London singlet or triplet functions and the Hamiltonian matrix of Eq. (15) correspondingly augmented with an additional row and column [19,20]. This implementation is equivalent to the development of Eqs. (16)–(19), but entails performing separate calculations for the singlet and triplet states in a manner which serves to accelerate the convergence of each individual calculation. In this way, accurate potential energy curves are obtained for the H_2 molecule which converge smoothly from their Heitler-London approximations to the essentially exact Kolos-Wolniewicz curves [26], providing further confidence in the development of Eqs. (16)–(19) [19,20].

Applications to weakly bound (van der Waals) atomic clusters provide useful first steps in implementation of the spectral-product method for many-electron atoms more generally. In the case of inert-gas clusters doped with a single optically active atomic radical, attention is focused on efficient construction of the individual Coulombic

atomic-radical/inert-gas pair-interaction matrices required in Eq. (15) [16]. In this approach, similar in spirit to atoms- and diatomics-in-molecules and related methods [14,15] but differing significantly in its implementation [16], a unitary transformation from diatomic to spectral-product representations is employed to decompose the adiabatic diatomic states and potential energy curves calculated employing standard methods [1,2] into diabatic-like atomic-product states and the associated interaction energy matrices of Eq. (15). Although successfully employed in "on-the-fly" constructions of ground and electronically excited potential energy surfaces in Monte Carlo and molecular dynamics simulations of singly doped inert-gas clusters [27], the absence of the transformation of Eqs. (16) to (19) in this approach for van der Waals clusters renders it unsuitable for more general applications involving, in particular, covalent and ionic bonding.

3.2 Atomic pair implementation

The particular form of the Hamiltonian matrix of Eq. (19) suggests the possibility of systematic evaluation of the individual atomic and interaction-energy terms appearing in Eq. (15), for which evaluations can be performed once and for all independent of any particular atomic aggregate arrangement, followed by construction of the aggregate-specific transformation matrix $\mathbf{U_P}(\boldsymbol{R})$ of Eq. (17). It is convenient for both pedagogical and notational simplicity to describe this approach for three interacting hydrogen atoms following the notation of Sect. 2.2, with the more general many-electron-atom case reported separately elsewhere [28].

In the three-atom case, the basis of Eq. (13) takes the form

$$\boldsymbol{\Phi}(\boldsymbol{r}:\boldsymbol{R}) = \left\{\boldsymbol{\phi}^{(a)}(\mathbf{1}) \otimes \boldsymbol{\phi}^{(b)}(\mathbf{2}) \otimes \boldsymbol{\phi}^{(c)}(\mathbf{3})\right\}_O , \tag{20}$$

where $\boldsymbol{R} = (\boldsymbol{R}_a, \boldsymbol{R}_b, \boldsymbol{R}_c)$ and $\boldsymbol{r} = (\mathbf{1}, \mathbf{2}, \mathbf{3})$ are the atomic and electronic coordinates, respectively. The corresponding Hamiltonian matrix of Eq. (19) includes three atomic terms and three atomic-pair interaction terms of the forms

$$\mathbf{H}_{\mathbf{P}}^{(\alpha)}(\boldsymbol{R}) \equiv \mathbf{U_P}(\boldsymbol{R})^{\dagger} \cdot \mathbf{H}^{(\alpha)} \cdot \mathbf{U_P}(\boldsymbol{R}) \tag{21}$$

$$\mathbf{V}_{\mathbf{P}}^{(\alpha,\beta)}(\boldsymbol{R}) \equiv \mathbf{U_P}(\boldsymbol{R})^{\dagger} \cdot \mathbf{V}^{(\alpha,\beta)}(\boldsymbol{R}_{\alpha\beta}) \cdot \mathbf{U_P}(\boldsymbol{R}), \tag{22}$$

where the atomic Hamiltonians $\mathbf{H}^{(\alpha)}$ in Eq. (21) ($\alpha = a, b,$ or c) are evaluated employing standard atomic spectral calculations [22].

In order to incorporate specifically diatomic calculations in evaluation of the atomic-pair interaction energy matrices $\mathbf{V}_{\mathbf{P}}^{(\alpha,\beta)}(\boldsymbol{R})$ of Eq. (22) ($\alpha\beta = ab, ac,$ or bc), the transformation matrix $\mathbf{U_P}(\boldsymbol{R})$ of Eq. (17) appearing there is factored [$\equiv \mathbf{U}_{\mathbf{P}}^{(\alpha,\beta)}(\boldsymbol{R}_{\alpha\beta}) \cdot \mathbf{U}_{\mathbf{P}}^{(T_{\alpha\beta})}(\boldsymbol{R})$] into two parts, where the unitary matrix $\mathbf{U}_{\mathbf{P}}^{(\alpha,\beta)}(\boldsymbol{R}_{\alpha\beta})$ diagonalizes the matrix representative $\mathbf{P}_{\mathbf{A}}^{(\alpha,\beta)}(\boldsymbol{R}_{\alpha\beta})$ of the two-electron antisymmetrizer constructed in the spectral-product basis of Eq. (20),

$$\begin{aligned}\mathbf{P}_{\mathbf{A}}^{(\alpha,\beta)}(\boldsymbol{R}_{\alpha\beta}) &\equiv \langle \boldsymbol{\Phi}(\boldsymbol{r}:\boldsymbol{R}) | \hat{P}_A^{(\alpha,\beta)}(2) | \boldsymbol{\Phi}(\boldsymbol{r}:\boldsymbol{R}) \rangle \\ &= \left\{\mathbf{p}_{\mathbf{A}}^{(\alpha,\beta)}(\boldsymbol{R}_{\alpha\beta}) \otimes \mathbf{I}^{(\gamma)}\right\}_O ,\end{aligned} \tag{23}$$

and the unitary matrix $\mathbf{U}_{\mathbf{P}}^{(T_{\alpha\beta})}(\boldsymbol{R})$ described further below completes the transformation from spectral-product to three-electron states of good permutation symmetry [Eq. (18)]. Evaluation of the matrix $\mathbf{P}_{\mathbf{A}}^{(\alpha,\beta)}(\boldsymbol{R}_{\alpha\beta})$ defined in Eq. (23) involves forming the outer product of the two-electron metric matrix $\mathbf{p}_{\mathbf{A}}^{(\alpha,\beta)}(\boldsymbol{R}_{\alpha\beta})$ with the unit matrix $\mathbf{I}^{(\gamma)}$ arising from the orthogonality of the third "by-stander" spin-orbital row vector, the elements of the resulting full matrix $\mathbf{P}_{\mathbf{A}}^{(\alpha,\beta)}(\boldsymbol{R}_{\alpha\beta})$ arranged in accordance with the ordering convention implied by the subscript "O" in Eq. (20) [16].

The transformation matrix $\mathbf{U}_{\mathbf{P}}^{(\alpha,\beta)}(\boldsymbol{R}_{\alpha\beta})$ that diagonalizes $\mathbf{P}_{\mathbf{A}}^{(\alpha,\beta)}(\boldsymbol{R}_{\alpha\beta})$ of Eq. (23) provides an intermediate "diatomic" basis set in the form [cf., Eq. (18)]

$$\begin{aligned}&\boldsymbol{\Phi}_{\mathbf{P}}^{(\alpha,\beta)}(\boldsymbol{r}:\boldsymbol{R}) \\ &\quad\equiv \boldsymbol{\Phi}(\boldsymbol{r}:\boldsymbol{R}) \cdot \mathbf{U}_{\mathbf{P}}^{(\alpha,\beta)}(\boldsymbol{R}_{\alpha\beta}) \\ &\quad= \left\{\{\boldsymbol{\phi}^{(\alpha)}(\boldsymbol{i}) \otimes \boldsymbol{\phi}^{(\beta)}(\boldsymbol{j})\} \cdot \mathbf{u}_{\mathbf{P}}^{(\alpha,\beta)}(\boldsymbol{R}_{\alpha\beta})\} \otimes \boldsymbol{\phi}^{(\gamma)}(\boldsymbol{k})\right\}_O \\ &\quad\rightarrow \left\{\{\boldsymbol{\Phi}_{\mathbf{P}}^{(\alpha,\beta)}(\boldsymbol{r}:\boldsymbol{R})\}_{p_{\alpha\beta}}, \{\boldsymbol{\Phi}_{\mathbf{P}}^{(\alpha,\beta)}(\boldsymbol{r}:\boldsymbol{R})\}_{u_{\alpha\beta}}\right\},\end{aligned} \tag{24}$$

where $\mathbf{u}_{\mathbf{P}}^{(\alpha,\beta)}(\boldsymbol{R}_{\alpha\beta})$ refers to the strictly diatomic portion of the transformation matrix $\mathbf{U}_{\mathbf{P}}^{(\alpha,\beta)}(\boldsymbol{R}_{\alpha\beta}) \equiv \{\mathbf{u}_{\mathbf{P}}^{(\alpha,\beta)}(\boldsymbol{R}_{\alpha\beta}) \otimes \mathbf{I}^{(\gamma)}\}_O$, the physical states $\{\boldsymbol{\Phi}_{\mathbf{P}}^{(\alpha,\beta)}(\boldsymbol{r}:\boldsymbol{R})\}_{p_{\alpha\beta}}$ are antisymmetric, the unphysical states $\{\boldsymbol{\Phi}_{\mathbf{P}}^{(\alpha,\beta)}(\boldsymbol{r}:\boldsymbol{R})\}_{u_{\alpha\beta}}$ are symmetric in the electron coordinates $\boldsymbol{i}$ and $\boldsymbol{j}$ in the closure limit, and the subscript $p_{\alpha\beta}$ ($u_{\alpha\beta}$) designates the dimension of the physical (unphysical) diatomic subspace. Note that designation of the basis states of Eq. (24) as "diatomic" refers to the specifically diatomic calculations required in their construction employing only the atomic-pair row vector $\{\boldsymbol{\phi}^{(\alpha)}(\boldsymbol{i}) \otimes \boldsymbol{\phi}^{(\beta)}(\boldsymbol{j})\}$, which diatomic states are subsequently augmented by multiplication with the third by-stander spin-orbital row vector $\boldsymbol{\phi}^{(\gamma)}(\boldsymbol{k})$, as indicated explicitly in the second line of Eq. (24) [16].

Employing the foregoing factoring $\mathbf{U_P}(\boldsymbol{R}) \equiv \mathbf{U}_{\mathbf{P}}^{(\alpha,\beta)}(\boldsymbol{R}_{\alpha\beta}) \cdot \mathbf{U}_{\mathbf{P}}^{(T_{\alpha\beta})}(\boldsymbol{R})$, the pairwise-atomic interaction-energy matrix of Eq. (22) can now be written in the form

$$\mathbf{V}_{\mathbf{P}}^{(\alpha,\beta)}(\boldsymbol{R}) \equiv \mathbf{U}_{\mathbf{P}}^{(T_{\alpha\beta})}(\boldsymbol{R})^{\dagger} \cdot \mathbf{V}_{\mathbf{P}}^{(\alpha,\beta)}(\boldsymbol{R}_{\alpha\beta}) \cdot \mathbf{U}_{\mathbf{P}}^{(T_{\alpha\beta})}(\boldsymbol{R}), \tag{25}$$

where the transformed interaction-energy matrix

$$\begin{aligned}\mathbf{V}_{\mathbf{P}}^{(\alpha,\beta)}(\boldsymbol{R}_{\alpha\beta}) &\equiv \mathbf{U}_{\mathbf{P}}^{(\alpha\beta)}(\boldsymbol{R}_{\alpha\beta})^{\dagger} \cdot \mathbf{V}^{(\alpha,\beta)}(\boldsymbol{R}_{\alpha\beta}) \cdot \mathbf{U}_{\mathbf{P}}^{(\alpha\beta)}(\boldsymbol{R}_{\alpha\beta}) \\ &= \langle \boldsymbol{\Phi}_{\mathbf{P}}^{(\alpha,\beta)}(\boldsymbol{r}:\boldsymbol{R}) | \hat{V}^{(\alpha,\beta)}(\boldsymbol{i},\boldsymbol{j}:\boldsymbol{R}_{\alpha\beta}) | \boldsymbol{\Phi}_{\mathbf{P}}^{(\alpha,\beta)}(\boldsymbol{r}:\boldsymbol{R}) \rangle\end{aligned} \tag{26}$$

is evaluated in the indicated permutation-symmetry-adapted diatomic basis of Eq. (24), and should not be confused with the matrix $\mathbf{V}_{\mathbf{P}}^{(\alpha,\beta)}(\boldsymbol{R})$ of Eq. (22) and the left-hand side of Eq. (25). Noting that the operator $\hat{V}^{(\alpha,\beta)}(\boldsymbol{i};\boldsymbol{j}:\boldsymbol{R}_{\alpha\beta})$ can be written as the difference of two diatomic Hamiltonian operators $[\hat{H}^{(\alpha,\beta)}(\boldsymbol{i},\boldsymbol{j}:\boldsymbol{R}_{\alpha\beta}) - \hat{H}^{(\alpha,\beta)}(\boldsymbol{i},\boldsymbol{j}:\boldsymbol{R}_{\alpha\beta}\rightarrow\infty)]$ which are symmetric functions of the electron coordinates $\boldsymbol{i}$ and $\boldsymbol{j}$, the matrix of Eq. (26) is seen to be block diagonal in the diatomic physical ($p_{\alpha\beta}$) and unphysical ($u_{\alpha\beta}$) labels, in accordance with Eq. (24).

The matrix $\mathbf{U}_{\mathbf{P}}^{(T_{\alpha\beta})}(\boldsymbol{R})$ required to complete the transformation of Eqs. (25) and (26) is obtained from diagonalization of the matrix representative

$$\begin{aligned}\mathbf{P}_{\mathbf{A}}^{(T_{\alpha\beta})}(\boldsymbol{R}) &\equiv \langle\boldsymbol{\Phi}_{\mathbf{P}}^{(\alpha,\beta)}(\boldsymbol{r}:\boldsymbol{R})|\hat{P}_A(3)|\boldsymbol{\Phi}_{\mathbf{P}}^{(\alpha,\beta)}(\boldsymbol{r}:\boldsymbol{R})\rangle \\ &= \mathbf{U}_{\mathbf{P}}^{(\alpha,\beta)}(\boldsymbol{R}_{\alpha\beta})^{\dagger}\cdot\mathbf{P}_{\mathbf{A}}(\boldsymbol{R})\cdot\mathbf{U}_{\mathbf{P}}^{(\alpha,\beta)}(\boldsymbol{R}_{\alpha\beta}) \qquad (27)\end{aligned}$$

of the three-electron antisymmetrizer $\hat{P}_A(3)$ constructed in the diatomic basis of Eq. (24), where $\mathbf{P}_{\mathbf{A}}(\boldsymbol{R})$ is its representation in the spectral-product basis of Eq. (20). Accordingly, it is clear from this expression that if $\mathbf{U}_{\mathbf{P}}^{(T_{\alpha\beta})}(\boldsymbol{R})$ diagonalizes $\mathbf{P}_{\mathbf{A}}^{(T_{\alpha\beta})}(\boldsymbol{R})$ of Eq. (27), the product matrix $\mathbf{U}_{\mathbf{P}}^{(\alpha\beta)}(\boldsymbol{R}_{\alpha\beta})\cdot\mathbf{U}_{\mathbf{P}}^{(T_{\alpha\beta})}(\boldsymbol{R})$ diagonalizes $\mathbf{P}_{\mathbf{A}}(\boldsymbol{R})$.

The three sets of three-electron permutation-symmetry-adapted states obtained from the foregoing development [cf., Eq. (18)],

$$\begin{aligned}\boldsymbol{\Phi}_{\mathbf{P}}^{(T_{\alpha\beta})}(\boldsymbol{r}:\boldsymbol{R}) &\equiv \boldsymbol{\Phi}_{\mathbf{P}}^{(\alpha,\beta)}(\boldsymbol{r}:\boldsymbol{R})\cdot\mathbf{U}_{\mathbf{P}}^{(T_{\alpha\beta})}(\boldsymbol{R}) \\ &= \boldsymbol{\Phi}(\boldsymbol{r}:\boldsymbol{R})\cdot\mathbf{U}_{\mathbf{P}}^{(\alpha\beta)}(\boldsymbol{R}_{\alpha\beta})\cdot\mathbf{U}_{\mathbf{P}}^{(T_{\alpha\beta})}(\boldsymbol{R}) \\ &\rightarrow \left\{\{\boldsymbol{\Phi}_{\mathbf{P}}^{(T_{\alpha\beta})}(\boldsymbol{r}:\boldsymbol{R})\}_p, \{\boldsymbol{\Phi}_{\mathbf{P}}^{(T_{\alpha\beta})}(\boldsymbol{r}:\boldsymbol{R})\}_u\right\}, \qquad (28)\end{aligned}$$

differ only in the sequence of permutation symmetry adaption employed in their construction. Accordingly, the functions of Eq. (28) are all equal to each other and to the defining states of Eq. (18) $[\boldsymbol{\Phi}_{\mathbf{P}}^{(T_{\alpha\beta})}(\boldsymbol{r}:\boldsymbol{R}) \rightarrow \boldsymbol{\Phi}_{\mathbf{P}}(\boldsymbol{r}:\boldsymbol{R})]$ in the limit of closure in Eqs. (24) and (27). In this limit, the three matrices $\mathbf{U}_{\mathbf{P}}^{(T_{\alpha\beta})}(\boldsymbol{R})$ can be conveniently obtained in the form $\mathbf{U}_{\mathbf{P}}^{(T_{\alpha\beta})}(\boldsymbol{R}) = \mathbf{U}_{\mathbf{P}}^{(\alpha\beta)}(\boldsymbol{R}_{\alpha\beta})^{\dagger}\cdot\mathbf{U}_{\mathbf{P}}(\boldsymbol{R})$, where the diatomic matrices $\mathbf{U}_{\mathbf{P}}^{(\alpha\beta)}(\boldsymbol{R}_{\alpha\beta})$ for $\alpha\beta = ab$, ac, or bc can each be constructed from an antisymmetrizer matrix $\mathbf{P}_{\mathbf{A}}^{(\alpha\beta)}(R_{\alpha\beta})$ which depends only upon the scalar separation $R_{\alpha\beta}$ employing standard angular-momentum considerations to provide the dependences upon the orientation of the vector separations $\boldsymbol{R}_{\alpha\beta}$ [16].

Finally, since the antisymmetrizer matrix of Eq. (27) is block diagonal in the diatomic labels $p_{\alpha\beta}$ and $u_{\alpha\beta}$ in the closure limit, the off-diagonal blocks $\{\mathbf{U}_{\mathbf{P}}^{(T_{\alpha\beta})}(\boldsymbol{R})\}_{u_{\alpha\beta}p_{\alpha\beta}}$ and $\{\mathbf{U}_{\mathbf{P}}^{(T_{\alpha\beta})}(\boldsymbol{R})\}_{p_{\alpha\beta}u_{\alpha\beta}}$ of the $\mathbf{U}_{\mathbf{P}}^{(T_{\alpha\beta})}(\boldsymbol{R})$ matrix vanish identically in this limit. Accordingly, the physical block of the interaction-energy matrix of Eq. (25) takes the form

$$\begin{aligned}\{\mathbf{V}_{\mathbf{P}}^{(\alpha,\beta)}(\boldsymbol{R})\}_{pp} = &\left\{\mathbf{U}_{\mathbf{P}}^{(T_{\alpha\beta})}(\boldsymbol{R})^{\dagger}\right\}_{pp_{\alpha\beta}}\cdot\left\{\mathbf{V}_{\mathbf{P}}^{(\alpha,\beta)}(\boldsymbol{R}_{\alpha\beta})\right\}_{p_{\alpha\beta}p_{\alpha\beta}} \\ &\cdot\left\{\mathbf{U}_{\mathbf{P}}^{(T_{\alpha\beta})}(\boldsymbol{R})\right\}_{p_{\alpha\beta}p}, \qquad (29)\end{aligned}$$

where $\{\mathbf{V}_{\mathbf{P}}^{(\alpha,\beta)}(\boldsymbol{R}_{\alpha\beta})\}_{p_{\alpha\beta}p_{\alpha\beta}}$ is the physical block of the interaction-enegy matrix of Eq. (26), and the the transformation matrix $\mathbf{U}_{\mathbf{P}}^{(T_{\alpha\beta})}(\boldsymbol{R})\}_{p_{\alpha\beta}p}$ is generally rectangular in view of the generally different dimensions of the physical subspaces $p_{\alpha\beta}$ and p ($\leq p_{\alpha\beta}$) of Eqs. (24) and (28), respectively. Equation (29) indicates that unphysical diatomic states do not contribute to the interaction terms, and that only the physical block $\{\mathbf{U}_{\mathbf{P}}^{(T_{\alpha\beta})}(\boldsymbol{R})\}_{p_{\alpha\beta}p}$ of the transformation matrix $\mathbf{U}_{\mathbf{P}}^{(T_{\alpha\beta})}(\boldsymbol{R})$ is required in the development.

A final expression for the physical block of the Hamiltonian matrix of Eq. (19) is obtained from the foregoing exact-atomic-pair development of Eqs. (20)–(29) in the form

$$\{\mathbf{H}_{\mathbf{P}}(\boldsymbol{R})\}_{pp} \equiv \sum_{\alpha=1}^{n}\left\{\{\mathbf{H}_{\mathbf{P}}^{(\alpha)}(\boldsymbol{R})\}_{pp} + \sum_{\beta=\alpha+1}^{n}\{\mathbf{V}_{\mathbf{P}}^{(\alpha,\beta)}(\boldsymbol{R})\}_{pp}\right\}, \qquad (30)$$

where the atomic terms are evaluated using Eq. (21) and the pair-interaction terms are given by Eq. (29) and the associated preceeding expressions.

3.3 Illustrative computational applications

Computational applications of the atomic-pair formalism reported here are based on the previously demonstrated general equivalence between the physical subspace of a spectral-product representation and the linearly independent canonically orthogonalized subspace of the associated explicitly antisymmetrized form of such a representation [20]. In a simple model illustration adopting this approach, the lowest lying doublet potential energy surfaces of the H_3 molecule are studied here in a minimal-basis-set representation [29,30].

The physical subspace of the diatomic states of Eq. (24), although formally defined in terms of the spectral-product representation of Eq. (20) employed there, is equivalently obtained in the present computational application from explicitly antisymmetric basis states in the familiar canonically orthogonalized form [20,21]

$$\begin{aligned}&\left\{\boldsymbol{\Phi}_{\mathbf{P}}^{(\alpha,\beta)}(\boldsymbol{r}:\boldsymbol{R})\right\}_{p_{\alpha\beta}} \rightarrow \\ &\frac{1}{\sqrt{2}}\{\hat{P}_A^{(\alpha,\beta)}(2)\,\boldsymbol{\Phi}(\boldsymbol{r}:\boldsymbol{R})\cdot\mathbf{U}_{\mathbf{P}}^{(\alpha,\beta)}(\boldsymbol{R}_{\alpha\beta})\}_{p_{\alpha\beta}} \\ &\cdot\{\mathbf{P}_{\mathbf{d}}^{(\alpha,\beta)}(\boldsymbol{R}_{\alpha\beta})\}_{p_{\alpha\beta}p_{\alpha\beta}}^{-1/2}, \qquad (31)\end{aligned}$$

where the transformation and eigenvalue matrices employed are obtained from the antisymmetrizer matrix $\mathbf{P}_{\mathbf{A}}^{(\alpha,\beta)}(\boldsymbol{R}_{\alpha\beta})$ of Eq. (23) given in the preceeding development. In turn, Eq. (31) is employed in evaluation of the physical blocks $\{\mathbf{V}_{\mathbf{P}}^{(\alpha,\beta)}(\boldsymbol{R}_{\alpha\beta})\}_{p_{\alpha\beta}p_{\alpha\beta}}$ and $\{\mathbf{P}_{\mathbf{A}}^{(T_{\alpha\beta})}(\boldsymbol{R})\}_{p_{\alpha\beta}p_{\alpha\beta}}$ of the interaction-energy and antisymmetrizer matrices of Eqs. (26) and (27), respectively, both of which are required in construction of the final expressions of Eqs. (29) and (30) for the atomic-pair form of the Hamiltonian matrix .

An expression similar to that of Eq. (31) can, of course, also be employed for the physical subspace of the aggregate states of Eq. (18) for H_3 in the form

$$\{\mathbf{\Phi}_{\mathbf{P}}(\boldsymbol{r}:\boldsymbol{R})\}_p \rightarrow \frac{1}{\sqrt{6}}\{\hat{P}_A(3)\,\mathbf{\Phi}(\boldsymbol{r}:\boldsymbol{R})\cdot\mathbf{U}_{\mathbf{P}}(\boldsymbol{R})\}_p\cdot\{\mathbf{P}_{\mathbf{d}}(\boldsymbol{R})\}_{pp}^{-1/2}, \tag{32}$$

where the indicated transformation and eigenvalue matrices are those of Eq. (17). Employing this expression in evaluating the Hamiltonian matrix in the usual variational approach gives rise to the multicenter integrals [29] the atomic-pair development is designed to avoid. That is, in contrast to Eq. (32), the atomic-pair expression for antisymmetric aggregate basis states is given by Eq. (28), in which only the diatomic states indicated there are made explicitly antisymmetric in accordance with Eq. (31), with the remaining antisymmetry in these functions accounted for in the limit by the indicated transformation matrix $\{\mathbf{U}_{\mathbf{P}}^{(T_{\alpha\beta})}(\boldsymbol{R})\}_{p_{\alpha\beta}p_{\alpha\beta}}$. Accordingly, it is seen that the atomic-pair implementation of the spectral-product approach can be expected to converge in the limit to results obtained from use of the valence-bond-like expression of Eq. (32), also taken to a suitable limit of convergence [30].

Adopting the foregoing approach in a minimal-basis-set description of the H_3 molecule, and restricting attention to $M_S = +1/2$ states, the spectral-product basis employed in Eq. (31) takes the three-term form

$$\mathbf{\Phi}(\boldsymbol{r}:\boldsymbol{R}) = 1s_a(1)1s_b(2)1s_c(3)\{\alpha(1)\alpha(2)\beta(3), \alpha(1)\beta(2)\alpha(3), \beta(1)\alpha(2)\alpha(3)\}, \tag{33}$$

where $\alpha(i)$ and $\beta(i)$ are the Pauli spin functions, and $1s_\alpha(i) \equiv 1s_\alpha(|\boldsymbol{r}_i - \boldsymbol{R}_\alpha|)$ refers to a $1s$ orbital centered on atom α. In this approximation, only the three indicated spin couplings contribute to the expressions of Eq. (20)–(30), with the diatomic interactions treated at the Heitler-London level of approximation spanning only the lowest lying singlet and triplet states.

The unitary transformation matrix of Eq. (16) in the representation of Eq. (33) is

$$\mathbf{P}_{\mathbf{A}}(\boldsymbol{R}) = \begin{pmatrix} 1-s_{ab}^2 & s_{ab}s_{ac}s_{bc}-s_{bc}^2 & s_{ab}s_{ac}s_{bc}-s_{ac}^2 \\ s_{ab}s_{ac}s_{bc}-s_{bc}^2 & 1-s_{ac}^2 & s_{ab}s_{ac}s_{bc}-s_{ab}^2 \\ s_{ab}s_{ac}s_{bc}-s_{ac}^2 & s_{ab}s_{ac}s_{bc}-s_{ab}^2 & 1-s_{bc}^2 \end{pmatrix}, \tag{34}$$

where $s_{\alpha\beta} = s(R_{\alpha\beta}) \equiv \langle 1s_\alpha(i)|1s_\beta(i)\rangle \leq 1$ is the one-electron $1s$ orbital overlap integral. The eigenvalue $\mathbf{P}_{\mathbf{d}}(\boldsymbol{R})$ and transformation $\mathbf{U}_{\mathbf{P}}(\boldsymbol{R})$ matrices of Eq. (17) are obtained from diagonalization of the matrix of Eq. (34) following the development of Eqs. (16)–(18) in the forms

$$\{\mathbf{P}_{\mathbf{d}}(\boldsymbol{R})\}_{1,2} = 1 - s_{ab}s_{bc}s_{ca} \pm \frac{1}{\sqrt{2}}\{(s_{ab}^2-s_{ac}^2)^2 + (s_{ab}^2-s_{bc}^2)^2 + (s_{ac}^2-s_{bc}^2)^2\}^{1/2} \tag{35a}$$

$$\{\mathbf{P}_{\mathbf{d}}(\boldsymbol{R})\}_3 = 1 - s_{ab}^2 - s_{ac}^2 - s_{bc}^2 + 2s_{ab}s_{bc}s_{ac}, \tag{35b}$$

and

$$\mathbf{U}_{\mathbf{S}}(\boldsymbol{R}) = \begin{pmatrix} \frac{1}{\sqrt{6}}\cos\Theta(\boldsymbol{R}) - \frac{1}{\sqrt{2}}\sin\Theta(\boldsymbol{R}) & \frac{1}{\sqrt{6}}\sin\Theta(\boldsymbol{R}) + \frac{1}{\sqrt{2}}\cos\Theta(\boldsymbol{R}) & \frac{1}{\sqrt{3}} \\ \frac{1}{\sqrt{6}}\cos\Theta(\boldsymbol{R}) + \frac{1}{\sqrt{2}}sin\Theta(\boldsymbol{R}) & \frac{1}{\sqrt{6}}\sin\Theta(\boldsymbol{R}) - \frac{1}{\sqrt{2}}\cos\Theta(\boldsymbol{R}) & \frac{1}{\sqrt{3}} \\ -\frac{2}{\sqrt{6}}\cos\Theta(\boldsymbol{R}) & -\frac{2}{\sqrt{6}}\sin\Theta(\boldsymbol{R}) & \frac{1}{\sqrt{3}} \end{pmatrix}, \tag{36a}$$

where

$$\Theta(\boldsymbol{R}) = \frac{1}{2}\tan^{-1}\left\{\frac{\sqrt{3}(s_{ab}^2-s_{ac}^2)}{(s_{ab}^2-2s_{bc}^2+s_{ac}^2)}\right\}. \tag{36b}$$

The two eigenvalues given by Eq. (35a) and the first two columns of the $\mathbf{U}_{\mathbf{P}}(\boldsymbol{R})$ matrix correspond to doublet states of H_3, whereas Eq. (35b) and the last column of $\mathbf{U}_{\mathbf{P}}(\boldsymbol{R})$ correspond to a quartet state, the functions of Eqs. (28) and (32) proving S=1/2, 3/2; $M_S = +1/2$ spin multiplets in this simple representation.

The corresponding diatomic antisymetrizer $\mathbf{P}_{\mathbf{A}}^{(\alpha,\beta)}(R_{\alpha\beta})$ and transformation $\mathbf{U}_{\mathbf{P}}^{(\alpha,\beta)}(R_{\alpha\beta})$ matrices of Eqs. (23) and (24), respectively, are obtained from appropriate limits of

Eqs. (34)–(36a), (36b) in the forms

$$\mathbf{P}_{\mathbf{A}}^{(a,b)}(R_{ab}) = \begin{pmatrix} 1-s_{ab}^2 & 0 & 0 \\ 0 & 1 & -s_{ab}^2 \\ 0 & -s_{ab}^2 & 1 \end{pmatrix}$$

$$\mathbf{U}_{\mathbf{P}}^{(a,b)}(R_{ab}) = \begin{pmatrix} 0 & 1 & 0 \\ \frac{1}{\sqrt{2}} & 0 & \frac{1}{\sqrt{2}} \\ -\frac{1}{\sqrt{2}} & 0 & \frac{1}{\sqrt{2}} \end{pmatrix}, \tag{37a}$$

$$\mathbf{P}_{\mathbf{A}}^{(a,c)}(R_{ac}) = \begin{pmatrix} 1 & 0 & -s_{ac}^2 \\ 0 & 1-s_{ac}^2 & 0 \\ -s_{ac}^2 & 0 & 1 \end{pmatrix}$$

$$\mathbf{U}_{\mathbf{P}}^{(a,c)}(R_{ac}) = \begin{pmatrix} \frac{1}{\sqrt{2}} & 0 & \frac{1}{\sqrt{2}} \\ 0 & 1 & 0 \\ -\frac{1}{\sqrt{2}} & 0 & \frac{1}{\sqrt{2}} \end{pmatrix}, \tag{37b}$$

$$\mathbf{P}_{\mathbf{A}}^{(b,c)}(R_{bc}) = \begin{pmatrix} 1 & -s_{bc}^2 & 0 \\ -s_{bc}^2 & 1 & 0 \\ 0 & 0 & 1-s_{bc}^2 \end{pmatrix}$$

$$\mathbf{U}_{\mathbf{P}}^{(b,c)}(R_{bc}) = \begin{pmatrix} \frac{1}{\sqrt{2}} & 0 & \frac{1}{\sqrt{2}} \\ -\frac{1}{\sqrt{2}} & 0 & \frac{1}{\sqrt{2}} \\ 0 & 1 & 0 \end{pmatrix}, \tag{37c}$$

and the eigenvalues of the three diatomic $\mathbf{P}_{\mathbf{A}}^{(\alpha\beta)}(R_{\alpha\beta})$ matrices all take the identical form

$$\mathbf{P}_{\mathbf{d}}^{(\alpha,\beta)}(R_{\alpha\beta}) = \mathbf{U}_{\mathbf{P}}^{(\alpha,\beta)}(R_{\alpha\beta})^{\dagger} \cdot \mathbf{P}_{\mathbf{A}}^{(\alpha,\beta)}(R_{\alpha\beta}) \cdot \mathbf{U}_{\mathbf{P}}^{(\alpha,\beta)}(R_{\alpha\beta}) = \begin{pmatrix} 1+s_{\alpha\beta}^2 & 0 & 0 \\ 0 & 1-s_{\alpha\beta}^2 & 0 \\ 0 & 0 & 1-s_{\alpha\beta}^2 \end{pmatrix}. \tag{38}$$

Construction of the diatomic states of Eq. (31) employing the $\mathbf{U}_{\mathbf{P}}^{(\alpha,\beta)}(R_{\alpha\beta})$ matrices of Eqs. (37a)–(37c) and the $\mathbf{P}_{\mathbf{d}}^{(\alpha,\beta)}(R_{\alpha\beta})$ matrix of Eq. (38) shows them to be products of antisymmetric Heitler-London diatomic states (ab, ac, or bc) of ${}^1\Sigma_g^+$ or ${}^3\Sigma_u^+$ symmetry with a by-stander $1s$ atomic spin orbital (c, b, or a) of appropriate electron spin.

In accordance with the discussion following Eq. (28), the transformation matrices required to evaluate Eq. (29) are obtained from the matrices of Eqs. (36a), (36b) and (37a)–(37c), which information completes evaluation of the Hamiltonian matrix of Eq. (30) for the H_3 molecule in a minimal-basis representation. In this case, the Hamiltonian can be written in a form that emphasizes the separate contributions from atomic energies and atomic-pair interaction potentials,

$$\mathbf{H}_{\mathbf{S}}(\boldsymbol{R}) = 3E_{1s}\mathbf{I} + \mathbf{U}_{\mathbf{S}}(\boldsymbol{R})^{\dagger} \cdot \mathbf{V}(\boldsymbol{R}) \cdot \mathbf{U}_{\mathbf{S}}(\boldsymbol{R}), \tag{39}$$

where the individual atomic-pair interaction terms have been combined into a total interaction-energy matrix of the form

$$\mathbf{V}(\boldsymbol{R}) \equiv \begin{pmatrix} {}^3V_{ab} + V_{ac}^{(av)} + V_{bc}^{(av)} & V_{bc}^{(diff)} & V_{ac}^{(diff)} \\ V_{bc}^{(diff)} & {}^3V_{ac} + V_{ab}^{(av)} + V_{bc}^{(av)} & V_{ab}^{(diff)} \\ V_{ac}^{(diff)} & V_{ab}^{(diff)} & {}^3V_{bc} + V_{ab}^{(av)} + V_{ac}^{(av)} \end{pmatrix}. \tag{40}$$

Here, ${}^3V_{\alpha\beta} \equiv {}^3V(R_{\alpha\beta})$ and ${}^1V_{\alpha\beta} \equiv {}^1V(R_{\alpha\beta})$ are the triplet and singlet Heitler-London interaction-energy curves, respectively, and $V_{\alpha\beta}^{(av)} \equiv [{}^3V(R_{\alpha\beta}) + {}^1V(R_{\alpha\beta})]/2$ is the average and $V_{\alpha\beta}^{(diff)} \equiv [{}^3V(R_{\alpha\beta}) - {}^1V(R_{\alpha\beta})]/2$ one-half the difference of these, all of which potentials vanish in the limit $R_{\alpha\beta} \to \infty$.

It is seen that the effect of the transformation matrix $\mathbf{U}_{\mathbf{S}}(\boldsymbol{R})$ in Eq. (39) is to modify the individual pairwise potentials of Eq. (40) to include non-pairwise-additive or three-body interactions in the Hamiltonian matrix, in common with earlier semi-empirical attempts to incorporate three-center terms in pair-interaction-based approximations to the H_3 molecule energy surface [31–36]. Detailed comparisons with these earlier approaches are of considerable interest, and are reported separately elsewhere [28]. Carrying out the indicated matrix multiplications in Eq. (39) shows that $\{\mathbf{H}_{\mathbf{S}}(\boldsymbol{R})\}_{13} = \{\mathbf{H}_{\mathbf{S}}(\boldsymbol{R})\}_{23} = 0$, as expected of Hamiltonian matrix elements connecting doublet and quartet states. Additionally, the element $\{\mathbf{H}_{\mathbf{S}}(\boldsymbol{R})\}_{12}$ is generally small, and vanishes identically in high-symmetry atomic arrangements [C_{2v}, $D_{\infty h}$, D_{3h}]. Of course, when the entire matrix of Eq. (39) is retained, its eigenvalues are identical with those obtained in the absence of the transformation matrix $\mathbf{U}_{\mathbf{S}}(\boldsymbol{R})$, whereas more generally only a small physical block of the transformed Hamiltonian is employed [Eq. (19)].

In the spirit of the blocking of Eq. (19), quantitative comparisons are provided here of the predictions of the two doublet-state diagonal elements of the model Hamiltonian matrix of Eqs. (39) and (40) with valence-bond calculations which include explicit three-center terms obtained from the representation of Eq. (32) [30]. The calculations performed employ a 12-term Gaussian representation of the $1s$ atomic hydrogen orbital which provides an orbital energy (-0.4999 au) in good agreement with the correct value, as well as explicitly antisymmetric singlet and triplet molecular hydrogen eigenstates and a ground-state equilibrium interatomic separation ($R_e = 1.642a_0$) and total energy (-1.1157 au) in good agreement with the accepted Heitler-London values [21].

Figure 1 shows contour plots of the two doublet eigenvalues of the $\mathbf{P}_{\mathbf{A}}(\boldsymbol{R})$ matrix of Eq. (34) obtained in the $1s^3$ H_3 representation for non-symmetric collinear atomic arrangements. Although the eigenvalues of the $\mathbf{P}_{\mathbf{A}}(\boldsymbol{R})$ matrix will converge in accordance with Eq. (17) in arbitrarily large basis sets, the minimal-basis results of Fig. 1 are nevertheless seen

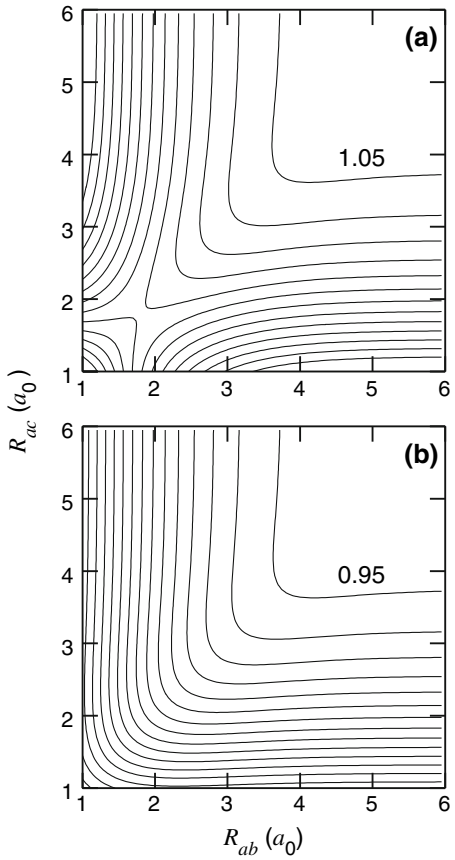

Fig. 1 Constant-value contours for the two doublet eigenvalues of the $\mathbf{P_A}(\boldsymbol{R})$ matrix of Eq. (34) for collinear atomic configurations of H_3 constructed in a $1s^3$ representation, employing an increment/decrement of 0.05 between adjacent contours. The coordinate axes give the distances R_{ab} and R_{ac} between the central atom located at the origin and the outer atoms, measured in atomic units (a_0). In **a** the contours increase uniformly in value from that labeled 1.05, except as $R_{ab} = R_{ac} \to 0$ inside the saddle point, in which region the values decrease monotonically to zero, whereas in **b** the contour values decrease uniformly from that labeled 0.95

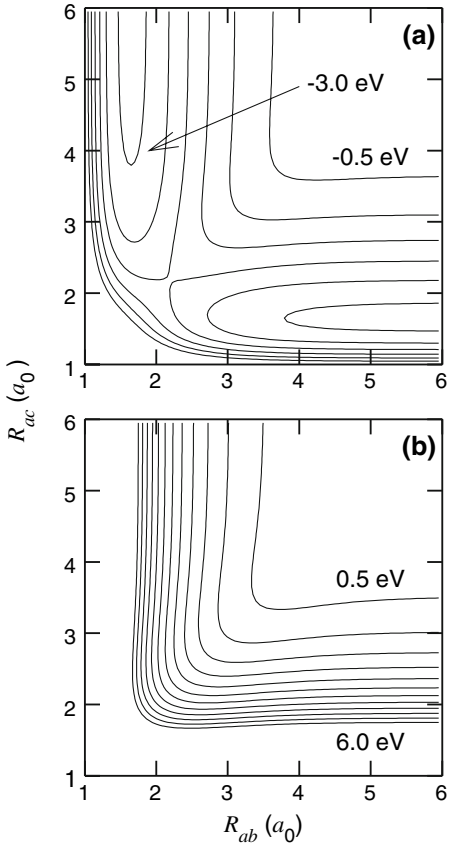

Fig. 2 Constant-energy contours for the ground- and first-excited doublet-state potential energy surfaces of H_3 for non-symmetric collinear atomic arrangements, obtained from Eqs. (39) and (40) constructed in a $1s^3$ representation, employing an energy decrement/increment of 0.5 eV between contours. The coordinate axes are as in Fig. 1, and the zero of energy employed (−1.50 au) is that of the three-atom dissociation limit (H + H + H). **a** depicts the familiar saddle and diatomic structures of the ground-state energy surface in H_3 [33], whereas the excited-state energy surface of **b** is montonically increasing with decreasing separations R_{ab} and/or R_{ac}

to provide qualitatively useful information. Specifically, the eigenvalue surface of Fig. 1a has a maximum along the line $R_{ab} = R_{ac}$ at 1.80 a_0, decreases rapidly to zero in the limit $R_{ab} = R_{ac} \to 0$, approaches 1 in the three-body break-up limit $R_{ab} = R_{ac} \to \infty$, and goes to 2 in the diatomic limits $R_{ab} \to 0$, $R_{ac} \to \infty$ and $R_{ab} \to \infty$, $R_{ac} \to 0$. The smaller doublet eigenvalue surface shown in Fig. 1(b) is evidently less structured than that of Fig. 1 (a) and vanishes in both the diatomic and triatomic united-atom limits. The vanishing of the eigenvalues of Fig. 1 as R_{ab} and $R_{ac} \to 0$ herald the formation of non-Pauli states in the representation of Eq. (33) or of linearly dependent doublet states in the representation of Eq. (32), indicating in either event that the minimal $1s^3$ basis does not support physically significant states in the united-atom limit $H_3 \to$ Li. The $\mathbf{P_A}(\boldsymbol{R})$-matrix eigenvalue surfaces evidently identify atomic configurations in which improper states arise, provide information complementary to the associated energy surfaces, and can anticipate the presence of crossings in the corresponding potential energy surfaces, as demonstrated in further detail below.

Figure 2 provides constant-energy contour plots of the two lowest lying doublet energy surfaces in H_3 obtained from Eqs. (39) and (40) for the non-symmetric collinear atomic arrangements of Fig. 1. These well-known energy surfaces are presented here to illustrate the extent of agreement obtained with corresponding conventional valence-bond calculations in a $1s^3$ basis [29,30], and to demonstrate their general accordance with accurate quantum-chemistry calculations [37–39]. Specifically, the calculated saddle-point energy (−1.574 au) of Fig. 2a compares well with that obtained from valence-bond calculations (−1.583au) in the same basis, and the H_3 saddle point geometry ($R_{ab} = R_{ac} = 2.18a_0$) is in general accord with the accepted position ($R_{ab} = R_{ac} = 1.757a_0$) [37–39]. The present calculation

places the saddle point approximately 0.0735 au (2.00 eV) below the three-body (H + H + H) breakup energy of −1.50au, and thus provides approximately 50% of the accepted accurate saddle-point binding energy of 0.1570 au (4.273 eV) relative to this limit [37–39]. The calculated saddle-point energy relative to the two-body break-up energy ($H + H_2$) provides a 1.14 eV barrier to the exchange reaction which is in accord with the valence-bond calculations (0.876 eV) but is about three times larger than the accepted value of 0.4166 eV [37–39], emphasizing the well-known sensitivity of this energy difference to the computational approximation employed [33].

The structure of the ground-state energy surface of Fig. 2a is evidently complementary to that of the associated $\mathbf{P_A}(\boldsymbol{R})$-matrix eigenvalue surface of Fig. 1a, with larger values of the $\mathbf{P_A}(\boldsymbol{R})$-matrix eigenvalues corresponding to generally lower energy values. Similarly, the energy surface for the excited doublet state shown in Fig. 2b is seen to be monotonically increasing from the three-atom break-up limit as the diatomic and triatomic united-atom limits are approached, complementary to the monotonically decreasing form of the associated $\mathbf{P_A}(\boldsymbol{R})$-matrix eigenvalue surface of Fig. 1b. The failure of the $1s^3$ representation to provide an accurate ground-state H_3 energy surface near the saddle point can be associated with the absence of physically significant states near the united-atom limit, as anticipated by the antisymmetrizer eigenvalue surfaces of Fig. 1.

In Fig. 3 are shown quantitative comparisons of the first two doublet energies in H_3 with corresponding three-center valence-bond calculations for symmetric collinear ($R_{ab} = R_{ac}$) atomic arrangements. Evidently, the results of Eqs. (39) and (40) for the ground-state energy surface are in good agreement with the $1s^3$ valence-bond calculations which include only covalent structures (○), and are also in accord with valence-bond results which include all possible ionic configurations (●) in the $1s^3$ basis [30]. The first excited doublet state in H_3 is seen to be repulsive, in good agreement with the valence-bond calculations and in qualitative accord with previously reported accurate calculations, although this excited doublet is known to undergo an avoided crossing with a higher lying state which is not included in the present development [40]. Although the results of Fig. 3 for the ground-state energy surface appear to bound the valence-bond results from above, this is only a happenstance. Indeed, similar apparent boundedness is not found for the excited doublet state in Fig. 3, although both results are in satisfactory agreement with the valence-bond calculations.

Figure 4 depicts contour plots of the two doublet-state $\mathbf{P_A}(\boldsymbol{R})$-matrix eigenvalues in H_3 for C_{2v} arrangements in which the $R_{ab} = R_{ac}$ separations are co-varied and the apex angle θ is varied from 30° to 180°. A seam of intersection of these two surfaces indicated by the cusps in the contours is evident in the figures at $\theta = 60°$, which corresponds to

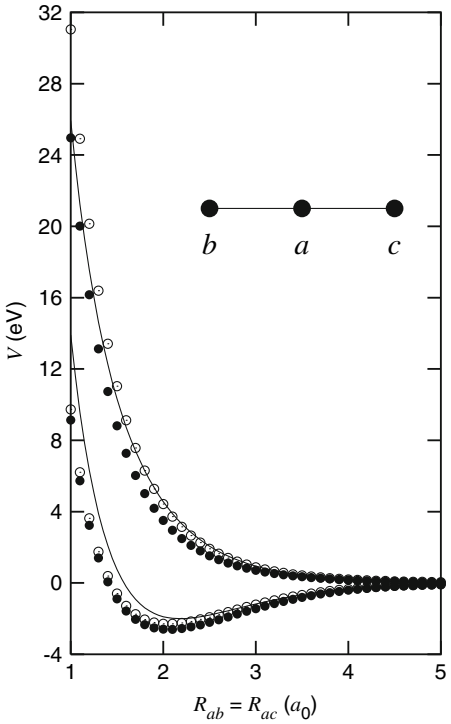

Fig. 3 Ground and first-excited doublet state energies in H_3 for symmetric collinear atomic arrangements. The *solid curves* depict the values obtained from Eqs. (39) and (40) constructed in a $1s^3$ representation, whereas the data points are obtained from conventional valence-bond calculations in a $1s^3$ basis set including (*filled circles*) and excluding (*open circles*) ionic configurations [30]. The zero of energy employed (−1.50 au) is that of the three-atom dissociation limit (H + H + H), as in Fig. 2

the familiar energy degeneracy associated with D_{3h} symmetry [33]. The dashed and solid portions of the contours in the two figures depict the continuous diabatic-like surfaces which pass smoothly through one another at the $\theta = 60°$ line of intersection, in accord with the degeneracy predicted by Eq. (35a). In panel (a) the higher value eigensurface (solid lines) is to the right of the 60° line and the lower value eigensurface (dashed lines) to the left of this line of intersection. Correspondingly, panel (b) shows the reversed arrangement, with the lower eigenvalue surface (dashed lines) to the right and the higher (solid lines) to the left of the 60° line.

The associated energy surfaces obtained from Eqs. (39) and (40) for the ground- and first-excited doublet states of H_3 for C_{2v} atomic arrangements, shown in Fig. 5, similarly depict the expected D_{3h} degeneracy at $\theta = 60°$ and the associated surface crossing along the cusps in the contours, complementary to the corresponding seam of intersection anticipated by the $\mathbf{P_A}(\boldsymbol{R})$-matrix eigenvalues of Fig. 4. This surface crossing arises in the present representation from the aforementioned vanishing of the off-diagonal Hamiltonian matrix element $\{\mathbf{H_S}(\boldsymbol{R})\}_{12}$ of Eqs. (39) and (40) at high symmetries.

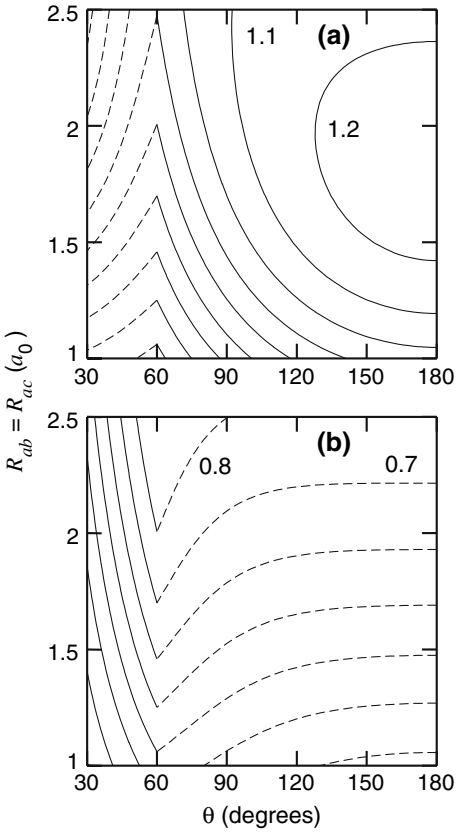

Fig. 4 Constant-value contours for the two doublet-state eigenvalues of the $\mathbf{P_A}(\boldsymbol{R})$ matrix of Eq. (34) constructed in a $1s^3$ representation for C_{2v} atomic arrangements ($R_{ab} = R_{ac}$), where θ is the apex angle of the triatomic H_3 configuration, employing an increment/decrement of 0.1 between adjacent contours. The cusps in the contours of both panels indicate the presence of a seam of intersection at $\theta = 60°$ in the two continuous surfaces identified by the *solid* and *dashed lines* corresponding to the two eigenvalues of Eq. (35a), with the contour values decreasing uniformly from right to left in **a** and decreasing uniformly from top to bottom in **b**, as discussed further in the text

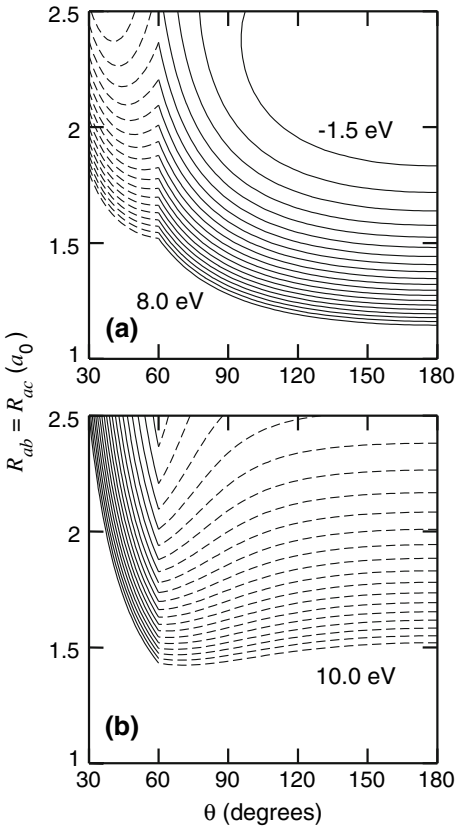

Fig. 5 Constant-energy contours for the two lowest lying doublet states of H_3 for C_{2v} atomic arrangements ($R_{ab} = R_{ac}$), obtained from Eqs. (39) and (40) constructed in a $1s^3$ representation, where θ is the apex angle of the triatomic configuration, employing an energy increment/decrement of 0.5 eV between adjacent contours. The zero of energy (−1.50au) is that of the three-atom dissociation limit (H + H + H). The cusps in the contours of both panels indicate the familiar D_{3h} symmetry seam of intersection at $\theta = 60°$ in the two continuous energy surfaces identified by the *solid* and *dashed lines* [33], with the contour energy values increasing uniformly from top to bottom in both panels. **a** depicts the lowest lying surface only for values of $\theta \geq 60°$, whereas **b** depicts the lowest lying surface only for $\theta \leq 60°$, as is discussed further in the text

In Fig. 6 are shown comparisons of the two lowest lying doublet energies in H_3 with coresponding valence-bond calculations for the C_{2v} atomic arrangements of Fig. 5 in which R_{ab} and R_{ac} are held fixed at the ground-state Heitler-London separation of 1.64 a_0 and θ is varied from 20° to 180°. Evidently, the present results are in good agreement with the corresponding three-center $1s^3$ valence-bond calculations which include only covalent structures (○). By contrast, although the present results are also in accord with valence-bond results which include all possible ionic configurations (●) in the $1s^3$ basis [30], the undulation between 120° and 180° evident upon inclusion of such terms in the valence-bond calculations is evidently not present in the $1s^3$ implementation of the atomic-pair formalism. The crossing of the two surfaces when $\theta = 60°$ is evident in the figure, and in accord with the valence-bond calculations. As in Fig. 3, the apparent upper bound provided by the present results on the valence-bond calculations in the case of the ground state in Fig. 6 is a happenstance, with a similar apparent upper boundedness not present in the case of the excited doublet state.

4 Concluding remarks

The theoretical development reported here provides an alternative perspective on electronic structure calculations for atoms and molecules and other forms of matter. Antisymmetry restrictions are enforced in this approach subsequent to construction of the many-electron Hamiltonian matrix of an atom or molecule in an orthogonal spectral-product basis. Transformation to a permutation-symmetry representation obtained from the eigenstates of the aggregate electron

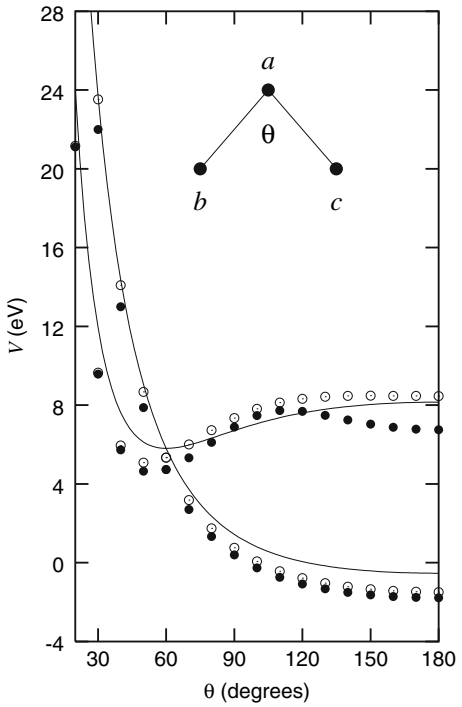

Fig. 6 Ground and first-excited doublet-state energies in H_3 for C_{2v} atomic arrangements ($R_{ab} = R_{ac} = 1.64a_0$), where θ is the apex angle of the triatomic configuration. The *solid curves* depict the values obtained from Eqs. (39) and (40) constructed in a $1s^3$ representation, whereas the data points are obtained from conventional valence-bond calculations in a $1s^3$ basis set including (*filled circles*) and excluding (*open circles*) ionic configurations [30]. The zero of energy (−1.50au) is that of the three-atom dissociation limit (H + H + H), as in Fig. 5. The crossing point of the two curves corresponds to D_{3h} symmetry, as discussed further in the text

antisymmetrizer enforces the requirements of the Pauli principle in this approach. Results are obtained in applications to many-electron atoms which are identical with the use of antisymmetrized configurational state functions in variational calculations, providing some degree of confidence in the soundness of the method more generally. In applications to the polyatomic molecules, the development accommodates the incorporation of fragment information in the form of Hermitian matrix representatives of atomic and diatomic operators which include the non-local effects of overall electron antisymmetry on the individual atomic and pairwise-atomic interaction terms.

Standard computational methods employing explicitly antisymmetric diatomic wave functrions are employed in constructing the pair-interaction matrices and other quantities required in an implementation of the method in the prototypically important H_3 molecule. The eigensurfaces of the matrix representative of the electron antisymmetrizer are seen to identify the presence of non-Pauli states in the representation employed, to complement the structures of the more familiar energy surfaces, and to anticipate the presence of seams of surface intersection associated with high-symmetry molecular geometries. The minimal-basis-set results reported provide energy surfaces in good agreement with corresponding three-center valence-bond calculations, and are in general accord with the results of accurate quantum-chemistry calculations.

The formalism reported avoids repeated calculations of the one- and two-electron many-centered integrals generally required in construction of polyatomic Hamiltonian matrices employing the antisymmetric basis states commonly adopted in calculations of potential energy surfaces. Rather, the approach entails atomic and molecular calculations which can be performed once and for all and retained for repeated applications, in combination with construction of an aggregate-specific transformation matrix designed to incorporate the non-local interaction effects associated with enforcement of complete electron antisymmetry. Accordingly, the present development can possibly provide an alternative *ab initio* approach suitable for computational applications to polyatomic molecules more generally.

Acknowledgments The financial support of the Air Force Research Laboratory, the US Air Force Office of Scientific Research, and the American Society of Engineering Education is gratefully acknowledged. We thank Drs. W. Kalliomaa, R. Channell, J.A. Sheehy, M. Fajardo, and G.A. Gallup for encouragement, support, assistance, and advice in various combinations and at various stages of the investigation, and the referees for very valuable comments.

References

1. Hoffmann MR, Dyall KG (eds) (2002) Low-lying potential energy surfaces. ACS Symposium Series 828, Washington, DC
2. Schmidt MW, Baldridge KK, Boatz JA, Elbert ST, Gordon MS, Jensen JH, Koseki S, Matsunaga N, Nguyen KA, Su SJ, Windus TL, Dupuis M, Montgomery JA (1993) J Comput Chem 14:1347
3. Pauli W (1925) Z Physik 31:765
4. Heisenberg W (1926) Z Physik 38:411
5. Heisenberg W (1926) Z Physik 39:499
6. Heisenberg W (1926) Z Physik 40:501
7. Dirac PAM (1926) Proc R Soc (London) A 112:661
8. Heisenberg W (1927) 41:239
9. Pauli W (1933) Allgemeine principien der wellenmechanik, vol 24, p 188, footnote 1. In: Handbuch der physik, Springer, Berlin
10. Dirac PAM (1958) The principles of quantum mechanics, 4th edn, chapter 9. Oxford University Press, New York
11. Pauli W (1980) General principles of quantum mechanics, p 116, footnote 1. Springer, Berlin
12. Eisenschitz H, London F (1930) Z Physik 60:491
13. Slater JC (1929) Phys Rev 34:1293
14. Moffitt W (1951) Proc R Soc (Lond) A 210:245
15. Ellison FO (1963) J Am Chem Soc 85:3540
16. Langhoff PW (1996) J Phys Chem 100:2974
17. Langhoff PW, Hinde RJ, Boatz JA, Sheehy JA (2002) Chem Phys Lett 358:231
18. Langhoff PW, Boatz JA, Hinde RJ, Sheehy JA (2002) Spectral theory of chemical bonding. In: Hoffmann MR, Dyall KG (eds) Low-lying potential energy surfaces, ACS Symposium Series 828, chapter 10. ACS, Washington, DC, pp 221–237

19. Langhoff PW, Boatz JA, Hinde RJ, Sheehy JA (2004) Applications of Löwdin's metric matrix: Atomic spectral methods for electronic structure calculations. In: Brändas E, Kryachko ES (eds) Fundamental world of quantum chemistry: a tribute to the memory of Per-Olov Löwdin, vol 3. Kluwer, Dordrecht, pp 97–114
20. Langhoff PW, Boatz JA, Hinde RJ, Sheehy JA (2004) J Chem Phys 121:9323
21. McWeeny R (1989) Methods of molecular quantum mechanics, 2nd edn. Academic, London
22. Condon EU, Shortley GH (1963) The theory of atomic spectra. University Press, Cambridge
23. Courant R, Hilbert D (1966) Methods of mathematical physics, vol 1, chapter 2. Interscience, New York
24. Hammermesh M (1962) Group theory. Addison-Wesley, Reading
25. Akhiezer NI, Glazman IM (1961) Theory of linear operators in Hilbert space, vol 1. Ungar, New York
26. Kolos W, Wolniewicz L (1965) J Chem Phys 43:2429
27. Spotts JM, Wong C-K, Johnson MS, Okumura M, Boatz JA, Hinde RJ, Sheehy JA, Langhoff PW (2003) J Phys Chem A 107:6948
28. Langhoff PW, Hinde RJ, Mills JD, Boatz JA (2007) J Chem Phys, in press
29. Slater JC (1931) Phys Rev 38:1109
30. Gallup GA (2002) Valence bond methods: theory and applications. Cambridge University Press, New York
31. Hirschfelder JO, Eyring H, Rosen H (1936) J Chem Phys 4:121
32. Ellison FO, Huff NT, Patel JC (1963) J Am Chem Soc 85:3544
33. Porter RN, Karplus M (1964) J Chem Phys 40:1105
34. Cashion JK, Herschbach DR (1964) J Chem Phys 40:2358
35. Eaker CW, Allard LR (1981) J Chem Phys 74:1821
36. Kleinkathöfer U, Tang KT, Toennies JP, Yiu CL (1999) J Chem Phys 111:3377
37. Siegbahn P, Liu B (1978) J Chem Phys 68:2457
38. Mielke SL, Garrett BC, Peterson KA (2002) J Chem Phys 116:4142
39. Peng Z, Kristyan S, Kuppermann A (1995) Phys Rev A 52:1005
40. Galster U, Baumgartner F, Müller U, Helm H, Jungen M (2005) Phys Rev A 72:062506